Thermochimica Acta 713 (2022) 179242

Contents lists available at ScienceDirect

Thermochimica Acta

journal homepage: www.elsevier.com/locate/tca

Thermal study of the hydrocalumite–katoite–calcite system

Alejandro Jiménez, Vicente Rives, Miguel A. Vicente *

GIR–QUESCAT, Departamento de Química Inorgánica, Universidad de Salamanca, E–37008 Salamanca, Spain

A R T I C L E I N F O

Keywords:
Hydrocalumite
Katoite
Calcite
Aluminum saline slag recovery
Microwaves aging
Thermal analyses

A B S T R A C T

Hydrocalumite ($Ca_2Al(OH)_6Cl{\cdot}2H_2O$) samples were prepared by the coprecipitation method, using Al^{3+} obtained from an aluminum slag, extracted in NaOH solutions and purified removing silica by precipitation with HCl. Hydrocalumite aging was assisted by microwave irradiation, and carried out under different temperatures. Very pure hydrocalumite was obtained under certain conditions, but samples impurified with katoite ($Ca_3Al_2(OH)_{12}$) and calcite ($CaCO_3$) were obtained in other cases. The thermal decomposition of hydrocalumite is complex and is not completely elucidated, compounds such as $Ca_{12}Al_{14}O_{33}$ (mayenite), Ca(OH)Cl and CaO have been proposed. The thermal characterization of this system was studied, also considering samples impurified with katoite and calcite, as a valuable and rapid method for identifying these phases.

1. Introduction

Metallurgy of aluminum is one of the most worldwide important industrial processes, due to the increasing consumption of this metal, related to its excellent properties for many applications [1]. The production of this metal combines ostentation from minerals and recycling of previously used aluminum. Recycling (leading to the so-called secondary aluminum) is well established and very extended in several countries. It consumes less energy than preparation of primary aluminum from its minerals, but it requires the addition of salts (mainly NaCl and KCl) for melting aluminum, finally generating an important waste, known as *Salt Cake or Saline Slag* [2]. This residue is hazardous [3], and various valorization procedures have been proposed, as its direct use as an adsorbent [4–6], but mainly its recovering, as sometimes it contains a large amount of aluminum [7], later used for the preparation of alumina [8], Layered Double Hydroxides (LDH) [9–12], or zeolites [13,14], among other materials. For this purpose, aluminum must be previously extracted, which, according to its amphoteric behavior, can be done both under acidic or alkaline conditions, and purified accordingly.

Following this strategy, we have recently reported the preparation of hydrocalumite from an aluminum slag [14]. Hydrocalumite ($Ca_2Al(OH)_6Cl{\cdot}2H_2O$) is a member of the Layered Double Hydroxides family [15], in which Ca^{2+} is the divalent cation, Al^{3+} the trivalent one, and chloride the interlayer anion. This solid has been widely used as an adsorbent [16], antacid [17], ion–exchanger [18], and basic heterogeneous catalyst [19–23]. Powder X–ray diffraction (PXRD) showed that, depending on the preparation conditions, pure hydrocalumite can be obtained, but in other cases the solids were impurified with katoite, a non–layered double hydroxide with formula $Ca_3Al_2(OH)_{12}$, and calcite ($CaCO_3$), which in some cases was only identified by Fourier-Transform infrared spectroscopy (FTIR) spectroscopy. In this context, thermal analyses can be a valuable and rapid method for identifying these phases. On the other hand, when reviewing the literature data on the thermal decomposition of hydrocalumite, certain aspects on its evolution at high temperature appeared to be unclear. The simplest decomposition route of this compound (dehydration followed by dehydroxylation would lead to formation of Ca_2AlO_3Cl in the penultimate step and removal of the interlayer anion, which under air or oxygen atmosphere, would led to $Ca_2AlO_{3.5}$ at the end of the process; however, formation of compounds such as $Ca_{12}Al_{14}O_{33}$ (mayenite), Ca(OH)Cl and CaO, have been proposed, while when Evolved Gas Analyses (EGA) was applied, discrepancies were observed on the emission of HCl or Cl_2O at high temperature (this will be analyzed in detail below in the discussion of the results). Thus, the thermal characterization of this system was studied, also considering samples impurified with katoite and calcite, as a valuable and rapid method for identifying these phases.

2. Experimental procedure

2.1. Materials

The method recently reported by us [14] to prepare hydrocalumite has been followed. We started from an aluminum slag kindly supplied by

* Corresponding author.
E-mail address: mavicente@usal.es (M.A. Vicente).

https://doi.org/10.1016/j.tca.2022.179242
Received 11 April 2022; Received in revised form 16 May 2022; Accepted 18 May 2022
Available online 20 May 2022

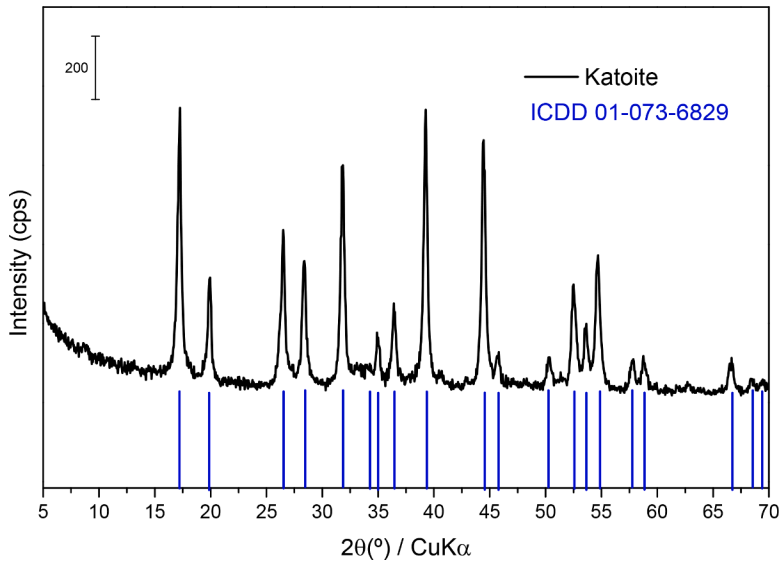

Fig. 1. Powder X–ray diffractogram of synthesized katoite, compared to the ICDD reference file for this compound.

IDALSA (Ibérica de Aleaciones Ligeras, Spain); after grinding and washing until obtaining a chloride-free solid, the fraction smaller than 0.4 mm was extracted with NaOH, as reported elsewhere [7], and the solution was treated with HCl 1 M to precipitate silicon-containing species as SiO_2; addition of $CaCl_2$ at pH 11.5 (fixed using NaOH) led to precipitation of a solid. Its treatment under microwave (MW) radiation in a Milestone Ethos Plus Microwave oven for 2 h at 125 or 130 °C led to formation of hydrocalumite, as identified by powder X-ray diffraction; however, treatments at 90–110 °C led to formation of a mixture of solid phases, namely, hydrocalumite, katoite and calcite. Synthetic hydrocalumite samples were named as MW-T, where T stands for the temperature (Celsius) of the microwave treatment; fore the calcined samples (see below), the calcination temperature (also in Celsius) was added to the name of the samples.

The method described by Sha et al. [24] was used to prepare pure katoite to be used as a reference material. A 2/1 molar ratio $Ca(OH)_2$ / $Al(OH)_3$ mixture was intimately mixed and grinded in a 250 mL stainless still mill jar (filled with 8 balls (20 mm diameter) and 10 balls (10 mm diameter) of the same material; balls/sample mass ratio was 36) for 3 h at 525 rpm in a PM100/200/CM (Retsch GmbH) planetary ball mill.

NaOH (technical grade and pharma grade), HCl (pharma grade, 37%) $CaCl_2$ (anhydrous, 95%), $CaCO_3$ calcite (analytical reagent), Ca $(OH)_2$ and $Al(OH)_3$ (analytical reagents) were from Panreac, while $CaCl_2{\cdot}2H_2O$ was supplied by Alfa Aesar (ACS 99–105%) and all were used as received, without any treatment.

2.2. Characterization techniques

A Siemens D-5000 equipment was used to record the powder X-ray diffraction (PXRD) patterns of the samples (λ = 0.154 nm Cu–Kα radiation, fixed divergence, 5° - 70° (2θ), scanning rate 2°(2θ)/min, 0.05° steps, 1.5 s/step). The crystalline phases formed were identified by comparison with the JCPDS database (International Centre for Diffraction Data, ICDD®) [25].

The thermogravimetric (TG) and Derivative Thermogravimetric (DTG) curves were recorded in a SDT Q600 apparatus (TA Instruments) at a heating rate of 2 °C/min up to 1350 °C and under oxygen (Air Liquide, Spain, 99.999%) flow (50 mL/min). The gaseous and vapor species formed during the thermal decomposition were analyzed (EGA, evolved gas analysis) by a mass spectrometer (Pfeiffer Vacuum ThermoStar TG–MS) connected to the thermal equipment.

Finally, characterization was completed by Scanning Electron Microscopy (SEM); the images were obtained using a JEOL IT500 Scanning Electron Microscope equipped with an Energy–Dispersive X–ray spectroscopy (EDS) microanalysis accessory, at the Nucleus Research Platform (University of Salamanca, Spain) facilities.

3. Results and discussion

3.1. Pure samples

3.1.a. Katoite

The PXRD diagram of synthesized katoite is shown in Fig. 1. Comparison with the ICDD file of this compound (card 01–073–6829)

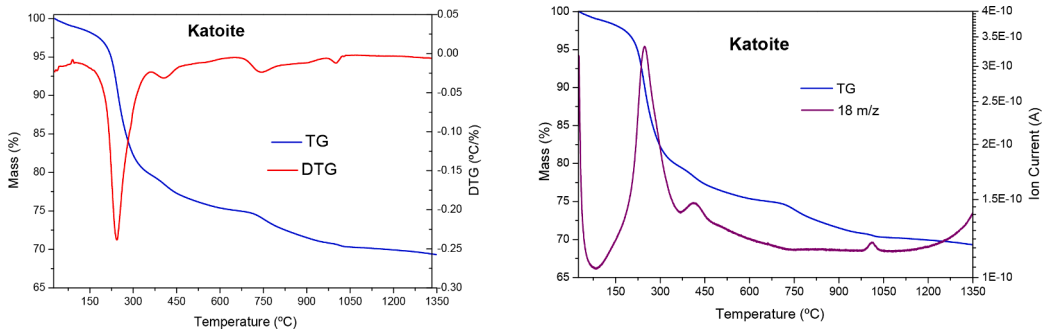

Fig. 2. Thermal curves of katoite: TG and DTG curves (left) and TG and EGA (H_2O) curves (right).

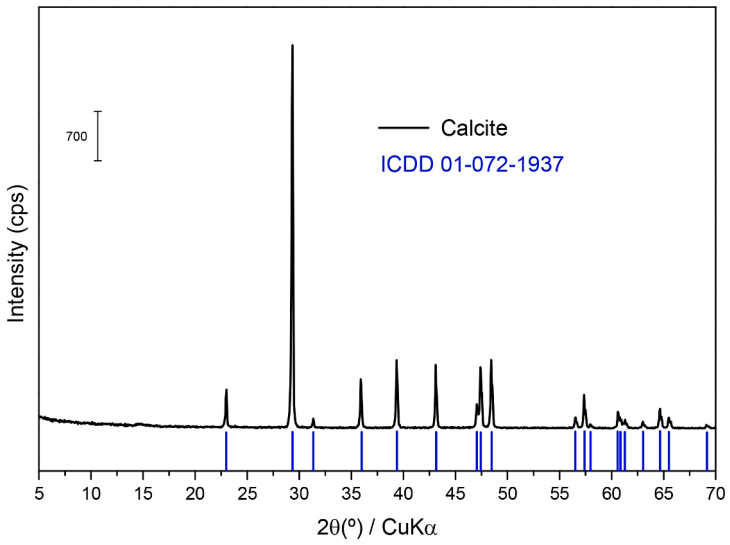

Fig. 3. Powder X–ray diffractogram of commercial calcite, compared to the ICDD reference file for this compound.

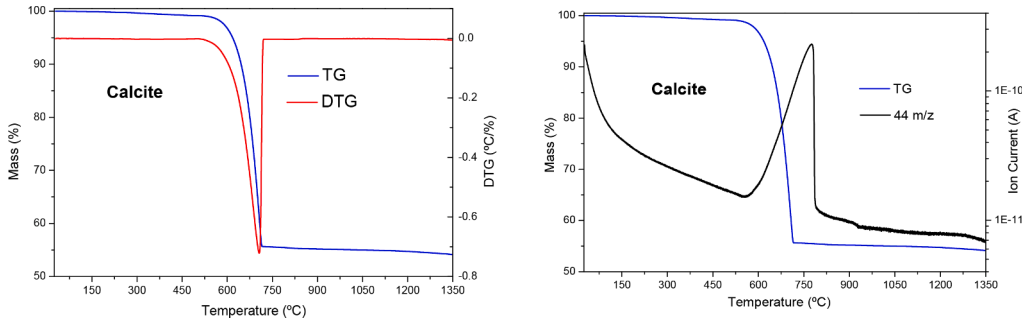

Fig. 4. Thermal curves of calcite: TG and DTG curves (left) and TG and EGA (CO_2) curves (right).

confirmed that the solid was composed of pure katoite. As expected, the crystallinity was not high as in other samples, considering that it was prepared by a simple mechanosynthesis procedure without any further heating treatment.

The thermal decomposition of katoite is shown in Fig. 2. The first process, due to the loss of weakly adsorbed water, began immediately upon starting the experiment, induced by the oxygen flow, losing a small amount of water at low temperature. Mass loss continued on heating, water being released from condensation of hydroxyl groups in a continuous process from 75 to 1100 °C, and the following equation may

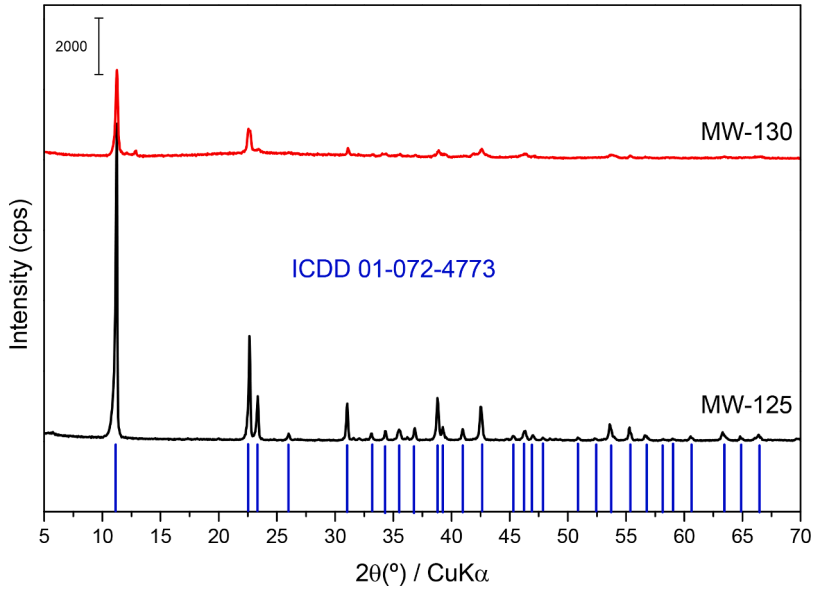

Fig. 5. Powder X–ray diffractogram of hydrocalumite samples, compared to the ICDD reference file for this compound.

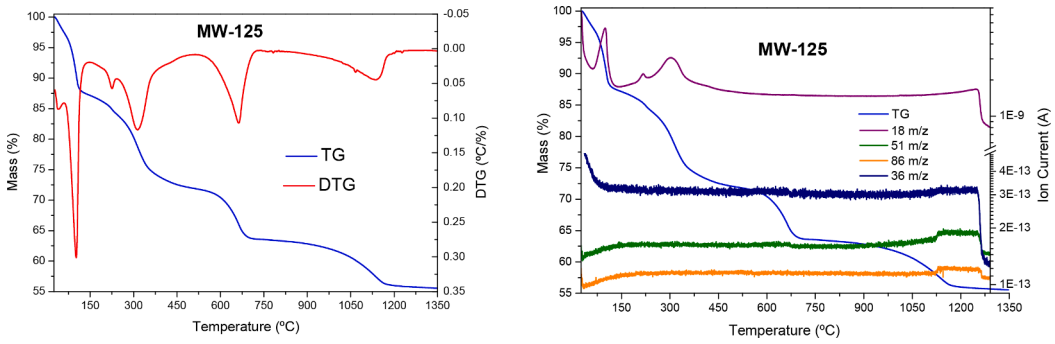

Fig. 6. Thermal curves of hydrocalumite: TG and DTG curves (left) and TG and EGA (CO_2, HCl and Cl_2O) curves (right).

be proposed:

$$Ca_3Al_2(OH)_{12}(s) \rightarrow Ca_3Al_2O_6(s) + 6H_2O(g) \quad (1)$$

The expected total mass loss according to this equation is 28.55% (4.76% for each water molecule formed), which agreed with the experimental result. Changes in the concavity of the curve were observed at approximately 250, 410, 750 and 1015 °C, in agreement with the minima shown in the DTG curve, the first process being much more intense than the others. Considering the mass loss caused by the removal of each water molecule, 4.76%, and the successive changes in the slope of the TG curve, removal of water took place in consecutive overlapped steps, the first one being the more intense (the relative intensity of the two peaks centered at 111 and 193 °C in the EGA curve was ca. 3). As it was expected, only water was detected when analyzing the gasses evolved upon the decomposition of this compound (Fig. 2).

3.1.b. *Calcite*

The PXRD diagram of commercial calcite is shown in Fig. 3. The solid showed a high crystallinity, with very intense and narrow diffraction peaks. Comparison with the ICDD file from this compound (card 01–072–1937) confirmed that the solid was composed of pure calcite.

The thermal curves for calcite are shown in Fig. 4. The behavior of this compound is well known, and the curves obtained confirmed this behavior, a single decomposition effect was observed, due to the reaction:

$$CaCO_3(s) \rightarrow CaO(s) + CO_2(g) \quad (2)$$

The single process was centered at 700 °C, with a mass loss coincident with the calculated value (43.96%). As expected, CO_2 was the only compound detected in the evolved gasses (Fig. 4).

3.1.c. *Hydrocalumite*

The purest hydrocalumite samples were obtained after microwave treatment at 125 °C and 130 °C, probably the small difference between these two temperatures made unappreciable any change in crystallinity in the PXRD diagrams; under other conditions, mixtures of hydrocalumite and katoite, and sometimes calcite, were obtained. The PXRD diagram of these solids exclusively showed the peaks due to hydrocalumite, ICDD card 01–072–4773 (Fig. 5), other phases were not detected, the only difference being the larger crystallinity (sharper and more intense diffraction maxima) for sample MW–125. For this reason, this sample was selected for further studies.

The thermal curves of this sample are shown in Fig. 6. The decomposition of this compound is usually claimed to occur by means of dehydration, dehydroxylation and removal of the interlayer anion [12,18,21,26]. Thus, removal of crystallization water followed by decomposition of the hydroxyl groups can be proposed, which may lead to the formation of the mixed oxychloride Ca_2AlO_3Cl, which under air or oxygen atmosphere should evolve to the mixed oxide $Ca_2AlO_{3.5}$, allowing to remove the chlorine atoms. This sequence would correspond the following equations:[1]

$$Ca_2Al(OH)_6Cl{\cdot}2H_2O(s) \rightarrow Ca_2Al(OH)_6Cl(s) + 2H_2O(g) \quad (3)$$

$$Ca_2Al(OH)_6Cl(s) \rightarrow Ca_2AlO_3Cl(s) + 3H_2O(g) \quad (4)$$

$$Ca_2AlO_3Cl(s) + 1/4O_2(g) \rightarrow Ca_2AlO_{3.5}(s) + 1/2Cl_2O(g) \quad (5)$$

Mixed oxychlorides and oxides have been reported at high temperature for other trivalent metals, such as Ca_2FeO_3Cl [23], and $Ca_2MO_{3.5}$ (*M*=Fe, Mn) [23,27]. However, up to our knowledge Ca_2AlO_3Cl and $Ca_2AlO_{3.5}$ have not been reported (actually, no references for these compounds were found at the JCPDS database). However, Renaudin et al. [28] have proposed the "empirical composition $Ca_4Al_2O_7$" (which is actually the same as $Ca_2AlO_{3.5}$) for the residue formed after heating of nitrate–hydrocalumite at 1300 °C (although the authors talked of empirical composition, not of formula of the compound). Tian and Guo [29] have reported the presence of $Ca_3Al_2O_6$ after heating at 1400–1500 °C, and it may be noted that the composition $Ca_4Al_2O_7$ may correspond to $Ca_3Al_2O_6$ (tricalcium aluminate) with segregation of CaO, and thus the simplest final composition of the residue would be $Ca_3Al_2O_6 + CaO$.

Regarding at the thermal curves, the first process was very fast and due to the dry oxygen atmosphere, dehydration began immediately at the beginning of the experiment. This process was completed at 110 °C, showing a concavity change at 115 °C; the mass loss, 12.0%, agreed with the calculated mass due to the removal of two water molecules from the formula of hydrocalumite, 12.8% (Eq. (3)).

The second mass loss, smoother than the first one, began immediately after the first one was completed. It ends around 400 °C, although it overlapped with the third process. The mass loss (27.5%) agreed with the removal of two water molecules (calculated loss 12.83%), in this case formed from partial dehydroxylation of hydrocalumite. The process can be divided into two steps, due to the presence of two different types of hydroxyl anions in the sheet, bonded to Ca^{2+} and Al^{3+} cations, respectively. In this sense, the formula of dehydrated hydrocalumite can be written as $Ca_2(OH)_4Al(OH)_2Cl$. Hydroxyl anions were more weakly bonded to Ca^{2+} than to Al^{3+}, resulting in FT–IR stretching bands at 3478 cm^{-1} (CaO—H bonds) and 3643 cm^{-1} (AlO—H bonds) (Fig. S1 and reference [12]). For this reason, two water molecules were first removed (from Ca^{2+}–bonded hydroxyls) and then one water molecule was removed (from Al^{3+}–bonded hydroxyls). In addition, this is in agreement with the concavity change in the TG curve and the endothermic peak at 230 °C in the DTG curve.

The third mass loss began, as indicated before, overlapping with the

[1] In the PDF version generated, Equations 3 and 5 are written in two lines. If possible, write them in one line.

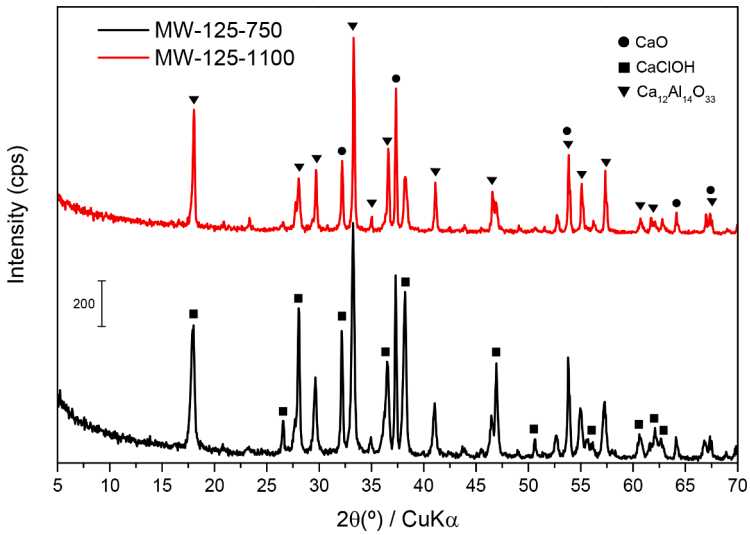

Fig. 7. Powder X–ray diffractogram of hydrocalumite calcined at 750 and 1100 °C.

previous process, and was completed at ca. 700 °C. The mass loss (36.5%) was compatible with the removal of one water molecule, thus completing the dehydroxylation of the compound leading to the corresponding oxychloride (calculated loss 6.42%). EGA showed the exclusive presence of water in the evolved gasses (Fig. 6). The processes were overlapped, and it was difficult to fix intervals of temperatures of stability of the intermediate compounds, but Eq. (4) can be divided into the following two Equations:

$$Ca_2Al(OH)_6Cl(s) \rightarrow Ca_2AlO_2(OH)_2Cl(s) + 2H_2O(g) \quad (4\text{–}1)$$

$$Ca_2AlO_2(OH)_2Cl(s) \rightarrow Ca_2AlO_3Cl(s) + H_2O(g) \quad (4\text{–}2)$$

A final mass loss occurred at high temperature, starting around 1000 °C, and it was completed at 1150 °C. According to the simple sequence above proposed, this process would correspond to the change from the oxychloride to the oxide, and thus it should imply the fixation of oxygen from the atmosphere, while chlorine atoms were released. In fact, the analyses of the evolved gasses showed that the chlorine atoms began to be removed at 1125 °C as Cl_2O; actually, the signals detected at $m/z = 86$ and 51 corresponded to Cl_2O and to its fragment ClO, which have been proposed to appear for the removal of Cl_2O [30]. Eq. (5) would explain the complete decomposition to the simplest compound, the mixed oxide $Ca_2AlO_{3.5}$. However, as indicated above, this mixed oxide has not been described for Al. In addition, the calculated total mass loss from hydrocalumite to this mixed oxide was 41.86%, while the experimental value was 44.5%, significantly different from the calculated value. In addition, the mass of the final residue did not coincide with that predicted if pure $Ca_2AlO_{3.5}$ was formed.

Several authors have studied the composition of the solid formed at high temperature in this system. For instance, formation of mayenite ($Ca_{12}Al_{14}O_{33}$), Ca(OH)Cl and CaO after heating at high temperature has been reported by several authors [29,31–34]. Grishchenko et al. [26] have proposed the presence of $Ca_{12}Al_{14}O_{32}Cl_2$ (formulated as $11CaO{\cdot}7Al_2O_3{\cdot}CaCl_2$), very similar to mayenite (the only difference is the substitution 1 oxide – 2 chlorides), underlying that both compounds were indistinguishable by PXRD. The removal of HCl has been reported at 1000 °C [35], but, in opposite, the decomposition of Ca(OH)Cl has also been proposed to occur at lower temperature, although in simple systems [36]. For gaining information on the phases existing after heating at high temperature, a portion of the solid was calcined at 750 °C in an open furnace for one hour, taking into account that thermogravimetry data suggested the existence of a stable phase between 700 and 850 °C because of the absence of any thermal effect in this temperature range. The diffractogram of the resulting solid (Fig. 7) showed a mixture of mayenite (ICDD card 98–000–5470), the hydroxychloride (Ca(OH)Cl), also formulated as CaClOH (ICDD card 98–000–8439), and CaO (ICDD card 98–002–1741), while, as indicated, comparison with Ca_2AlO_3Cl could not be carried out as no file for this compound was found at the JCPDS database. In order to evaluate the calculated mass of the observed mixture of phases, its composition was estimated by the RIR (Reference Intensity Ratio) method [37–39]. The RIR parameters used were those reported in the ICDD files for these compounds (2.07 for mayenite, 4.20 for CaO and 2.97 for Ca(OH)Cl), obtaining a phase composition 60.4% mayenite, 11.7% CaO and 27.9% Ca(OH)Cl. Amorphous phases were not expected after the calcination at this so high temperature and, interestingly, mayenite was the only crystalline phase containing aluminum. Under these premises, the simplest equation for decomposition of hydrocalumite to these phases should be:

$$14Ca_2Al(OH)_6Cl{\cdot}2H_2O(s) \rightarrow Ca_{12}Al_{14}O_{33}(s) + 2CaO(s) + 14Ca(OH)Cl(s) + 63H_2O(g) \quad (6)$$

The calculated mass loss involved in this reaction was 28.9%, while the mass loss up to 750 °C in the TG curve was 36.5%. On comparing the phase composition by transforming the mole ratio given in Eq. 6 into mass composition, the phase relation became 49.6% mayenite, 4.0% CaO and 46.3% Ca(OH)Cl, far from the composition calculated above. A possible explanation for this difference may be that XRD is a semi–quantitative technique, and may be affected by the differences in the growing of the crystals and the intensity of the peaks of these phases when forming together under calcination, and not as pure compounds used in the ICDD cards for calculating their RIR parameters. However, the observed difference may have alternatively another possible explanation, based on the removal of HCl. This reaction would be:

$$14Ca_2Al(OH)_6Cl{\cdot}2H_2O(s) \rightarrow Ca_{12}Al_{14}O_{33}(s) + 16CaO(s) + 14HCl(g) + 63H_2O(g) \quad (7)$$

This reaction implies a larger mass loss, due to the decomposition of the hydroxychloride evolving HCl (compare with Eq. 6), a reaction suggested to occur in the last step of the thermal decomposition of hydrocalumite [34,35]. Comparing the mass loss at 750 °C in Fig. 6 with Eqs. 6 and 7, it seemed that decomposition of hydrocalumite was halfway between the processes described in these equations. Thus, as indicated above, if decomposition of hydrocalumite occurred up to Eq. 6, the mass loss should be 28.9% the solid residue amounting 71.1% of the initial sample mass, while if decomposition advanced up to complete Eq. 7, the mass loss should be 41.9%, with a solid residue of 48.1%; however, the experimental values were 36.5% and 63.5, respectively. Thus, it seemed that Eq. 7 had begun to occur but has not been

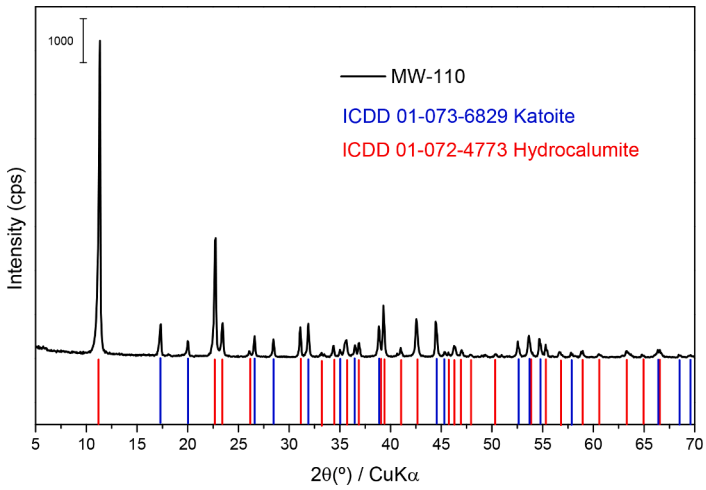

Fig. 8. Powder X–ray diffractogram of sample MW–110, compared to the ICDD reference files for hydrocalumite and katoite.

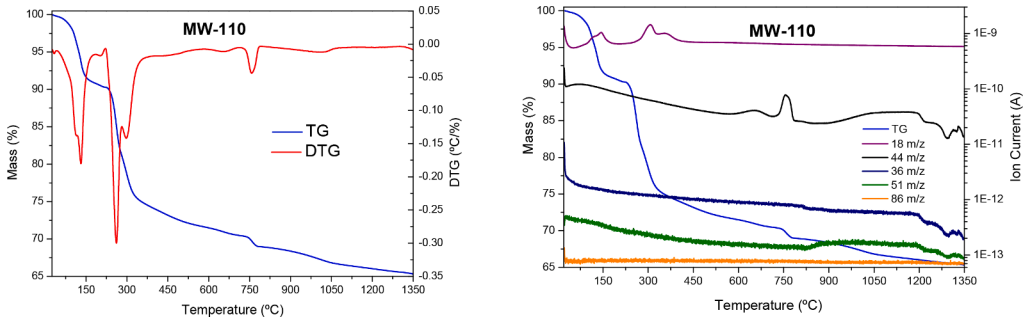

Fig. 9. Thermal curves of MW–110 solid: TG and DTG curves (left) and TG and EGA (CO_2, HCl and Cl_2O) curves (right).

completed. In fact, the removal of HCl was clearly suggested from the EGA results in Fig. 6 (notice the very weak increase at high temperature, >1000 °C, in the intensity of the $m/z = 36$ signal in the mass spectrum), although the result was not conclusive due to the precision of our equipment. If it is accepted that Ca_2AlO_3Cl is the single phase formed after hydrocalumite dehydroxylation, HCl would not be removed because of the absence of available H atoms. Formation of the hydroxychloride suggested in Eq. 6 and its further decomposition satisfactorily explained the emission of HCl in Eq. 7, together with that of Cl_2O under an oxidant atmosphere.

For gaining information on the nature of the final solid, a portion of the solid was calcined at 1100 °C in an open furnace (unfortunately we could not calcine it at higher temperature). The diffractogram of the resulting solid calcined at 1100 °C was very similar to that of the solid calcined at 750 °C, showing the presence of the phases above indicated, only with small differences in the relative intensity of their peaks (Fig. 7). As a summary, the phases are the same at 750 and 1100 °C, only observing a decrease of the intensity of CaClOH at higher temperature. Again, the absence of a reference card for $Ca_2AlO_{3.5}$ avoided any reliable straight comparison with this possible phase. On the other hand, the presence of CaO became obvious, and taking into account that the Ca:Al ratio in hydrocalumite (2) is higher than in most of the mixed oxides formed by these elements, the formation of other mixed oxides with segregation of CaO is tentatively suggested. In any case, the "intermediate" phases (mayenite, hydroxychloride) were very stable, and formation of the final phases was difficult. Rossi et al. (2019) [34] remarked the difficulty for detecting HCl, underlying the high energy involved in its release and thus the difficulty for decomposition of Ca(OH)Cl.

3.2. Synthetic hydrocalumites

As stated above, the synthesis of hydrocalumite was, in general, successful, once the conditions of extraction of aluminum from the slag and the procedure to obtain hydrocalumite from the extracted liquors were established in previous works [7,12]. However, in some cases, the samples showed the presence of other phases. As a representative example, the solid prepared by MW treatment at 110 °C was selected, as its powder X–ray diffraction diagram showed the presence of katoite in addition to hydrocalumite (Fig. 8); carbonate bands were detected by FTIR spectroscopy, suggesting also the presence of calcite, that was not detected by PXRD, probably because it was present in a very little amount and widely dispersed throughout the solid [12].

The thermal curves of this sample are shown in Fig. 9. These curves can be seen as the superposition of those of hydrocalumite (Fig. 6) and katoite (Fig. 2). Water was removed in processes centered at 130 °C (with a shoulder at 114 °C), 260 and 297 °C (determined by the minima in the DTG curve) (Fig. 9), and the TG curve resembled a sum of those from the pure compounds. In addition, a clear mass loss was observed at 735–780 °C, which strongly suggested the presence of calcite, confirmed by the EGA curve of CO_2 ($m/z = 44$, peak centered at 751 °C), although this phase had not been previously detected by powder X–ray diffraction. The mass loss associated to this effect was 1.3%, which allowed to estimate the amount of calcite in the sample as 2.9%. As expected, the mass of the final residue, 65.3%, was intermediate between the mass of the residue derived from the calcination of the pure compounds separately. This allowed to estimate the composition of the original solid, that resulted 60% hydrocalumite, 37.1% katoite, and 2.9% calcite. It may be remarked here that quantification of this solid by PXRD was avoided by the usual preferential orientation in layered hydrocalumite particles.

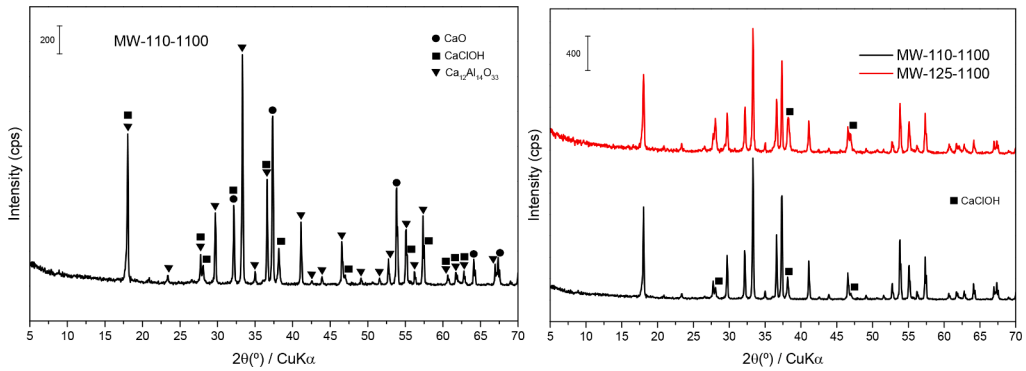

Fig. 10. Powder X–ray diffractogram of sample MW–110 calcined at 1100 °C (left) and comparison with sample MW–125 calcined at 1100 °C (right), where the most intense peaks from CaClOH are labeled.

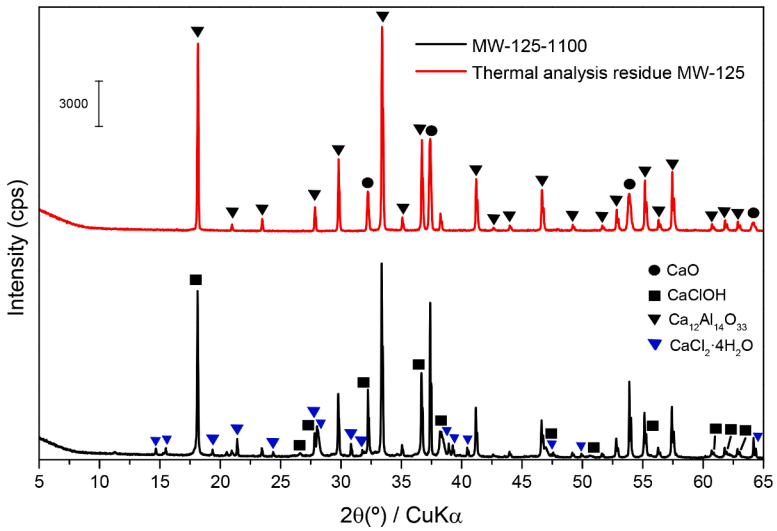

Fig. 11. Powder X–ray diffractogram of hydrocalumite calcined at 1100 °C in an open furnace and at 1350 °C in the thermal analyses apparatus.

The presence of katoite and calcite should influence the thermal behavior of hydrocalumite; to insight in this point, sample MW–110 was also calcined at 1100 °C, and the powder X–ray diffractogram of the residue was recorded. This residue was composed of mayenite, CaClOH and CaO (Fig. 10) and its comparison with pure hydrocalumite calcined at the same temperature showed the intensity of the peaks from CaClOH as the only difference (Fig. 10). The lower intensity of the peaks due to this compound in sample MW–110 may be simply due to the lower content of hydrocalumite (as katoite and calcite do not contain chlorine and do not produce CaClOH on decomposition), but it is also possible that the presence of these admixtures induces the decomposition of the hydroxychloride at a lower temperature.

3.3. Study of the residue formed after calcination of hydrocalumites at 1350 °C

The results above reported encouraged us to study more in detail the products of the calcination of hydrocalumite at high temperature. The residue from the thermal analyses was collected and submitted to powder X–ray diffraction analysis (notice that this residue had been calcined to 1350 °C). A slower scan speed was applied, and the powder X-ray diffractogram of the solid calcined in the open furnace at 1100 °C was also recorded under the same conditions, for comparison (Fig. 11).

The diffractograms were very similar to each other, both samples contained mayenite and CaO as the main components. However, two important differences were observed: First, the intensity of the peaks from CaClOH, decreased on increasing the calcination temperature from 1100 to 1350 °C, which may suggest that evolution of HCl progressed in this temperature range. However, the presence of $CaCl_2{\cdot}4H_2O$ (ICDD file 01–072–1015) was clearly detected in the solid calcined at 1350 °C. The presence of such a hydrated compound was not expected after calcination at a so high temperature, but it may be considered that $CaCl_2$ is highly hygroscopic [40], so if anhydrous $CaCl_2$ was formed under calcination it may hydrate during the handling for PXRD registration. In fact, formation of $CaCl_2$ (hydrophilite) has been reported by Tian and Guo after heating at 1400–1500 °C (in their case, the anhydrous phase was found, the authors remarked that the calcined solids were cooled "in a container previously filled with allochroic silica gel as desiccant") [29], but such a caution was not taken in our case. The presence of $CaCl_2$ strongly suggests that not all interlayer chloride ions escaped and some of them were combined with calcium in the original hydrocalumite structure to form hydrophilite or calcium chloride hydroxide.

Formation of $CaCl_2$ may occur by segregation from the mayenite-like phase $Ca_{12}Al_{14}O_{32}Cl_2$, but it may also be formed from hydroxychloride by means of the following reaction (Eq. (8)):

$$2CaOHCl(s) \rightarrow CaO(s) + CaCl_2(s) + H_2O(s) \quad (8)$$

This decomposition route for CaOHCl may not evolve HCl, but led to formation of $CaCl_2$, a compound which presence was previously only suggested by Tian and Guo [29]. In addition, this route implied the removal of water at very high temperature. Returning to Fig. 6, evolution of water seemed to occur at 1200 °C, although the result was not

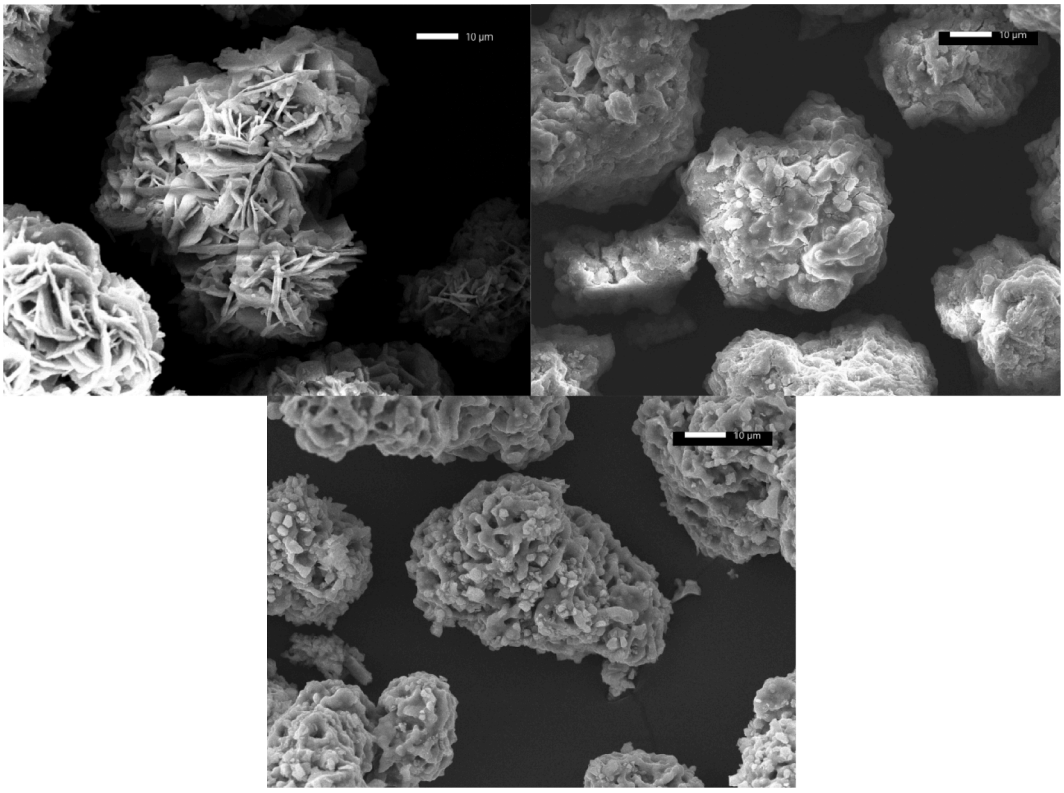

Fig. 12. SEM micrographs of MW-125 solid after heating at 700 °C (up, left), at 1100 °C (up, right) and residue after thermal analyses finishing at 1350 °C (down). The bar scale represents a length of 10 µm in all micrographs.

conclusive.

On the other hand, related to the formation of $CaCl_2$, it may be remarked that, in spite of its strong ionic character, the easy volatility of this compound has been reported [41]). This was now investigated by carrying out its thermal analyses under the same conditions used for the other solids (Fig. S2). The initial dehydration was observed at low temperature, perfectly agreeing with the calculated mass loss (24.5%), followed by melting of the compound, detected by an endothermal effect at 778 °C (tabulated melting point, 772 °C [40]). Once melted, the volatilization of this compound was observed as a gentle effect from ca. 800–1300 °C. Although the amount of $CaCl_2$ in the residue of hydrocalumite may be low, and its volatility may be different when dispersed in a matrix mainly composed of mayenite, this effect may not be ruled out to occur also in our sample, contributing to the total mass loss observed.

The evolution of this solid was also investigated by SEM. The micrographs (Fig. 12) showed clear differences as a function of the temperature; the micrographs of the samples calcined at 750 °C were typical of mayenite, the solids became spongier at higher temperature, suggesting the formation of new phases. The EDS analyses (Fig. S3 and S4, Supplementary Material) showed that Cl was present in high amounts up to 1100 °C, but strongly decreasing at 1350 °C, in accordance with PXRD results. Almost Cl–free particles very low Al content seemed to correspond to segregated CaO (see point Spc_005), supporting the formation of this compound by the final decomposition reactions.

4. Conclusion

The thermal behavior of synthetic hydrocalumite ($Ca_2Al(OH)_6Cl{\cdot}2H_2O$) has been studied. As the synthesis of this compound implied the possible formation of katoite ($Ca_3Al_2(OH)_{12}$) and calcite ($CaCO_3$), all these compounds were studied. The decomposition of hydrocalumite was complicated. Although a simple process leading to the mixed oxychloride Ca_2AlO_3Cl and finally to the mixed oxide $Ca_2AlO_{3.5}$ has been proposed in the literature, the process is much more complex. Formation of mayenite ($Ca_{12}Al_{14}O_{33}$), CaOHCl and CaO was observed, the hydroxychloride being stable up to high temperature, explaining the difficulties reported in the literature to detect HCl in the evolved gasses. Even more, formation of $CaCl_2$ (observed as its hydrated phase by PXRD, due to the hygroscopicity of this compound) was detected after calcination at 1350 °C, suggesting a new decomposition route, in which the hydroxychloride decomposed to CaO and $CaCl_2$, without emission of HCl.

Declaration of Competing Interest

The authors declare that they have no known competing financial interests or personal relationships that could have appeared to influence the work reported in this paper.

Acknowledgements

Financial support from Universidad de Salamanca (Plan I-B2). AJ thanks Universidad de Salamanca and Banco Santander for a predoctoral contract.

CRediT authorship contribution statement

This work is a section of the Ph. D. Thesis of AJ, supervised by VR and MAV. By this reason, AJ was the author mostly involved in the experimental part of the work and in the elaboration of the results (Data curation, Formal analysis, Investigation, Methodology, Writing original draft, Writing review & edition), always under the supervision of VR and MAV (Conceptualization, Funding acquisition, Methodology, Resources, Validation, Writing review & edition).

Supplementary materials

Supplementary material associated with this article can be found, in the online version, at doi:10.1016/j.tca.2022.179242.

References

[1] World Bureau of Metal Statistics, http://www.world-bureau.com/ (2020).
[2] A. Gil, Management of the salt cake from secondary aluminum fusion processes, Ind. Eng. Chem. Res. 44 (2005) 8852–8857, https://doi.org/10.1021/ie050835o.
[3] Directive 2010/75/EU of the European Parliament and of the Council, of 24 November 2010, on industrial emissions (integrated pollution prevention and control). 2010. Official Journal of the European Union, 17.12.2010, L 334/17.
[4] A. Gil, S. Albeniz, S.A. Korili, Valorization of the saline slags generated during secondary aluminum melting processes as adsorbents for the removal of heavy metal ions from aqueous solutions, Chem. Eng. J. 251 (2014) 43–50, https://doi.org/10.1016/j.cej.2014.04.056.
[5] A. Gil, S.A. Korili, Management and valorization of aluminum saline slags: current status and future trends, Chem. Eng. J. 289 (2016) 74–84, https://doi.org/10.1016/j.cej.2015.12.069.
[6] A. Gil, E. Arrieta, M.A. Vicente, S.A. Korili, Application of industrial wastes from chemically treated aluminum saline slags as adsorbents, ACS Omega 3 (2018) 18275–18284, https://doi.org/10.1021/acsomega.8b02397.
[7] A. Jiménez, V. Rives, M.A. Vicente, A. Gil, A comparative study of acid and alkaline aluminum extraction valorization procedure for aluminum saline slags, J. Environ. Chem. Eng. 10 (2022), 107546, https://doi.org/10.1016/j.jece.2022.107546.
[8] B.R. Das, B. Dash, B.C. Tripathy, I.N. Bhattacharya, S.C. Das, Production of η–alumina from waste aluminum dross, Miner. Eng. 20 (2007) 252–258, https://doi.org/10.1016/j.mineng.2006.09.002.
[9] A. Gil, E. Arrieta, M.A. Vicente, S.A. Korili, Synthesis and CO_2 adsorption properties of hydrotalcite–like compounds prepared from aluminum saline slag wastes, Chem. Eng. J. 334 (2018) 1341–1350, https://doi.org/10.1016/j.cej.2017.11.100.
[10] L. Santamaría, M. López–Aizpún, M. García–Padial, M.A. Vicente, S.A. Korili, A. Gil, Zn–Ti–Al layered double hydroxides synthesized from aluminum saline slag wastes as efficient drug adsorbents, Appl. Clay Sci. 187 (2020), 105486, https://doi.org/10.1016/j.clay.2020.105486.
[11] L. Santamaría, M.A. Vicente, S.A. Korili, A. Gil, Saline slag waste as an aluminum source for the synthesis of Zn–Al–Fe–Ti layered double–hydroxides as catalysts for the photodegradation of emerging contaminants, J. Alloys Compd. 843 (2020), 156007, https://doi.org/10.1016/j.jallcom.2020.156007.
[12] A. Jiménez, A. Misol, Á. Morato, V. Rives, M.A. Vicente, A. Gil, Optimisation of hydrocalumite preparation under microwave irradiation for recovering aluminum from a saline slag, Appl. Clay Sci. 212 (2021), 106217, https://doi.org/10.1016/j.clay.2021.106217.
[13] M. Yoldi, E.G. Fuentes–Ordoñez, S.A. Korili, A. Gil, Zeolite synthesis from industrial wastes, Micropor. Mesopor. Mater. 287 (2019) 183–191, https://doi.org/10.1016/j.micromeso.2019.06.009.
[14] A. Jiménez, A. Misol, A. Morato, V. Rives, M.A. Vicente, A. Gil, Synthesis of pollucite and analcime zeolites by recovering aluminum from a saline slag, J. Clean. Prod. 297 (2021), 126667, https://doi.org/10.1016/j.jclepro.2021.126667.
[15] V. Rives, Layered Double Hydroxides, Nova Science Publishers, 2001.
[16] Y. Takaki, X. Qiu, T. Hirajima, K. Sasaki, Removal mechanism of arsenate by bimetallic and trimetallic hydrocalumites depending on arsenate concentration, Appl. Clay Sci. 134 (2016) 26–33, https://doi.org/10.1016/j.clay.2016.05.010.
[17] C.F. Linares, J. Moscosso, V. Alzurutt, F. Ocanto, P. Bretto, G. González, Carbonated hydrocalumite synthesized by the microwave method as a possible antacid, Mater. Sci. Eng. C 61 (2016) 875–878, https://doi.org/10.1016/j.msec.2016.01.007.
[18] N. Murayama, I. Maekawa, H. Ushiro, T. Miyoshi, J. Shibata, M. Valix, Synthesis of various layered double hydroxides using aluminum dross generated in aluminum recycling process, Int. J. Miner. Process 110–111 (2012) 46–52, https://doi.org/10.1016/j.minpro.2012.03.011.
[19] J. Granados–Reyes, P. Salagre, Y. Cesteros, Effect of the preparation conditions on the catalytic activity of calcined Ca/Al–layered double hydroxides for the synthesis of glycerol carbonate, Appl. Catal. A 536 (2017) 9–17, https://doi.org/10.1016/j.apcata.2017.02.013.
[20] J. Granados–Reyes, P. Salagre, Y. Cesteros, G. Busca, E. Finocchio, Assessment through FT–IR of surface acidity and basicity of hydrocalumites by nitrile adsorption, Appl. Clay Sci. 180 (2019), 105180, https://doi.org/10.1016/j.clay.2019.105180.
[21] M. Rosset, O.W. Perez–Lopez, Cu–Ca–Al catalysts derived from hydrocalumite and their application to ethanol dehydrogenation, React. Kinet. Mech. Catal. 126 (2019) 497–511, https://doi.org/10.1007/s11144-018-1513-y.
[22] R.L. Souza Júnior, T.M. Rossi, C. Detoni, M.M.V.M. Souza, Glycerol carbonate production from transesterification of glycerol with diethyl carbonate catalyzed by Ca/Al–mixed oxides derived from hydrocalumite, Biomass Conv. Bioref. (2020), https://doi.org/10.1007/s13399-020-01110-4.
[23] M. Szabados, A.A. Ádám, P. Traj, S. Muráth, K. Baán, P. Bélteky, Z. Kónya, Á. Kukovecz, P. Sipos, I. Pálinkó, Mechanochemical and wet chemical syntheses of CaIn–layered double hydroxide and its performance in a transesterification reaction compared to those of other $Ca_2M(III)$ hydrocalumites (M: Al, Sc, V, Cr, Fe, Ga) and Mg(II)–, Ni(II)–, Co(II)– or Zn(II)–based hydrotalcites, J. Catal. 391 (2020) 282–297, https://doi.org/10.1016/j.jcat.2020.07.038.
[24] L. Sha, Z. Zou, J. Qu, X. Li, Y. Huang, C. Wu, Z. Xu, As(III) removal from aqueous solution by katoite ($Ca_3Al_2(OH)_{12}$), Chemosphere 260 (2020), 127555, https://doi.org/10.1016/j.chemosphere.2020.127555.
[25] ICDD Database, JCPDS–International Centre for Diffraction Data (ICDD®), 2020. Newtown Square, PA, USA.
[26] R.O.Grishchenko, A.L. Emelina, P.Y. Makarov, Thermodynamic properties and thermal behavior of Friedel's salt, Thermochim. Acta 570 (2013) 74–79, https://doi.org/10.1016/j.tca.2013.07.030.
[27] H.I. Saleh, Synthesis and formation mechanisms of calcium ferrite compounds, J. Mater. Sci. Technol. 20 (2004) 530–534.
[28] G. Renaudin, J.-.P. Rapin, B. Humbert, M. François, Thermal behaviour of the nitrated AFm phase $Ca_4Al_2(OH)_{12}(NO_3)_2 \cdot 4H_2O$ and structure determination of the intermediate hydrate $Ca_4Al_2(OH)_{12}(NO_3)_2 \cdot 2H_2O$, Cem. Concr. Res. 30 (2000) 307–314, https://doi.org/10.1016/S0008-8846(99)00251-3.
[29] J. Tian, Q. Guo, Thermal decomposition of hydrocalumite over a temperature range of 400–1500 °C and its structure reconstruction in water, J. Chem. (2014) 1–8, https://doi.org/10.1155/2014/454098.
[30] NIST Standard Reference Data, US National Institute of Standards and Technology, 2022 (Available at: https://webbook.nist.gov/chemistry/form-ser/).
[31] M.J. Campos–Molina, J. Santamaría–Gonźalez, J. Ḿerida–Robles, R. Moreno–Tost, M.C.G. Albuquerque, S. Bruque–Ǵamez, E. Rodríguez–Castellón, A. Jiménez–López, P. Maireles–Torres, Base catalysts derived from hydrocalumite for the transesterification of sunflower oil, Energy Fuels 24 (2010) 979–984, https://doi.org/10.1021/ef9009394.
[32] E. Pérez–Barrado, M.C. Pujol, M. Aguiló, J. Llorca, Y. Cesteros, F. Díaz, J. Pallarès, L.F. Marsal, P. Salagre, Influence of acid–base properties of calcined MgAl and CaAl layered double hydroxides on the catalytic glycerol etherification to short–chain polyglycerols, Chem. Eng. J. 264 (2015) 547–556, https://doi.org/10.1016/j.cej.2014.11.117.
[33] L. Zheng, S. Xia, Z. Hou, Hydrogenolysis of glycerol over Cu–substituted hydrocalumite mediated catalysts, Appl. Clay Sci. 118 (2015) 68–73, https://doi.org/10.1016/j.clay.2015.09.002.
[34] T.M. Rossi, J.C. Campos, M.M.V.M. Souza, An evaluation of calcined hydrocalumite as carbon dioxide adsorbent using thermogravimetric analysis, Appl. Clay Sci. 182 (2019), 105252, https://doi.org/10.1016/j.clay.2019.105252.
[35] M. Domínguez, M.E. Pérez–Bernal, R.J. Ruano–Casero, C. Barriga, V. Rives, R.A. S. Ferreira, L.D. Carlos, J. Rocha, Multiwavelength luminescence in lanthanide–doped hydrocalumite and mayenite, Chem. Mater. 23 (2011) 1993–2004, https://doi.org/10.1021/cm200408x.
[36] K.M. Allal, J.C. Dolignier, G. Martin, Determination of thermodynamical data of calcium hydroxichloride, Oil Gas Sci. Technol. – Rev. IFP 52 (1997) 361–368, https://doi.org/10.2516/ogst:1997046.
[37] F.H. Chung, Quantitative interpretation of X–ray diffraction patterns of mixtures. I. Matrix–flushing method for quantitative multicomponent analysis, J. Appl. Cryst. 7 (1974) 519–525, https://doi.org/10.1107/S0021889874010375.
[38] F.H. Chung, Quantitative interpretation of X–ray diffraction patterns of mixtures. II. Adiabatic Principle of X–ray diffraction analysis of mixtures, J. Appl. Cryst. 7 (1974) 526–531, https://doi.org/10.1107/S0021889874010387.
[39] F.H. Chung, Quantitative interpretation of X–ray diffraction patterns of mixtures. III. Adiabatic Simultaneous determination of a set of reference intensities, J. Appl. Cryst. 8 (1975) 17–19, https://doi.org/10.1107/S0021889875009454.
[40] R. Kemp, S.E. Keegan, Calcium Chloride. In Ullmann's Encyclopedia of Industrial Chemistry, Wiley Online Library, 2000, https://doi.org/10.1002/14356007.a04_547.
[41] R.G. Bautista, J.L. Margrave, The heat of sublimation of calcium chloride, J. Phys. Chem. 67 (1963) 2411–2412, https://doi.org/10.1021/j100805a036.